### Title

Characteristics of dimeric (bis) bidentate selective high affinity ligands as HLA-DR10 beta antibody mimics targeting non-Hodgkin's lymphoma




### Journal

International Journal of Oncology, 31(4)

### ISSN

1019-6439



### Authors

DeNardo, Gerald L
Hok, Saphon
Van Natarajan, Arutselvan
et al.



### Publication Date

2007-10-01

Peer reviewed

# Characteristics of dimeric (bis) bidentate selective high affinity ligands as HLA-DR10 beta antibody mimics targeting non-Hodgkin's lymphoma

GERALD L. DeNARDO[1], SAPHON HOK[2], ARUTSELVAN NATARAJAN[1], MONIQUE COSMAN[2], SALLY J. DeNARDO[1], FELICE C. LIGHTSTONE[2], GARY R. MIRICK[1], AINA YUAN[1], JULIE PERKINS[2], VLADIMIR V. SYSKO[1], JOERG LEHMANN[1] and RODNEY L. BALHORN[2]

[1]University of California Davis Cancer Center, Sacramento, CA;
[2]Lawrence Livermore National Laboratories, Livermore, CA, USA

Received May 14, 2007; Accepted July 2, 2007

*'Yesterday is history, tomorrow is a mystery, and today is a gift; that's why they call it the present'* -Eleanor Roosevelt

**Abstract.** Despite their large size, antibodies have proven to be suitable radioisotope carriers to deliver systemic radiotherapy, often molecular image-based, for lymphoma and leukemia. To mimic antibody (Ab) targeting behavior while decreasing size by 50-100x, a combination of computational and experimental methods were used to generate molecules that bind to unique sites within the HLA-DR epitopic region of Lym-1, an Ab shown effective in patients. Lym-1 Ab mimics (synthetic high afinity ligands; SHALs) were generated and studied *in vitro*, using live cell binding assays, and/or pharmacokinetic studies over 24 h in xenografted mice given 1 or 20 $\mu$g SHAL doses i.v. Multimilligram amounts of each of the dimeric (bis) SHALs were synthesized at high purity, and labeled with indium-111 at high specific activity and purity. These SHALs were selective for HLA-DR and HLA-DR expressing malignant cells and had functional affinities that ranged from $10^{-9}$ M (nanomolar) to $10^{-10}$ M. Blood clearances ranged from 3.6 to 9.5 h and body clearances ranged from 15.2 to 43.0 h for the 6 bis DOTA-SHALs studied in a mouse model for non-Hodgkin's lymphoma (NHL). While localization was shown in Raji NHL xenografts, biodistribution was influenced by 'sinks' for individual ligands of the SHALs. Highly pure, dimeric mimics for HLA-DR Ab were synthesized, biotinylated and radiolabeled, and showed selectivity *in vitro*. Pharmacokinetic behavior in mice was influenced by the ligands and by the linker length of the dimeric SHALs. Nanomolar or better functional affinity was observed when a suitably long linker was used to connect the two bidentate SHALs. The concept and methodology are of interest because applicable for targeting most proteins; the SHAL synthetic platform is highly efficient and adaptive.

*Correspondence to:* Dr Gerald L. DeNardo, Radiodiagnosis and Therapy Molecular Cancer Institute, 1508 Alhambra Blvd., Room 3100, Sacramento, CA 95816, USA
E-mail: gldenardo@ucdavis.edu

*Key words:* antibodies, leukemia, lymphoma, nanomolecules, imaging, treatment

## Introduction

The use of Abs as therapeutics has grown rapidly (1). Radioimmunotherapy (RIT), often molecular imaging-based, has proven to be effective for NHL, providing a several-fold increase in response rates when compared to immunotherapy or to 'salvage' chemotherapy, and greater patient acceptance (2,3). As well as Abs perform, however, there is an opportunity for improvements. Abs are macromolecules that penetrate vascular and tumor barriers poorly and interact with a variety of receptors, limiting their selectivity as radioisotope carriers and adding to their adverse event profile. Abs have a long residence time in the circulation that contributes to dose-limiting toxicity when they are conjugated to radioisotopes (4).

Small molecules, e.g. chemotherapy drugs, penetrate but also exit cancer quickly, unless bound in the cancer; these drugs also penetrate cancer more completely. Other small drugs, e.g., fluorine-18 deoxyglucose used for positron emission tomography and iodine-131 sodium iodide used for thyroid cancer imaging and therapy, are bound in the cancer. We adopted a blueprint for boosting the targeting index of molecular imaging and therapy, using novel, small molecules to mimic the highly specific binding of Abs through multiple contacts with their protein target (5). Two or more molecules (referred to as ligands) that bind to sites on the protein can be linked together to produce multidentate molecules that bind with higher affinity than the original ligands (5-7). If the ligands and connecting linkers are selected properly, it is highly improbable that identical docking sites will be found on another protein separated by the same distances. SHALs have been designed to detect anthrax, a potential weapon for bioterrorism (8). SHALs designed to bind to a discrete epitopic region of an antigen and having a size less than one fiftieth that of a whole Ab, can be referred to as 'Ab mimics'. SHALs better fulfill the potential of molecular targeting by

more closely mimicking the behavior of $^{131}$I-iodide in thyroid cancer, the paradigm for radioisotopic molecular imaging and therapy (Fig. 1). $^{131}$I-iodide is a small molecule radioisotope carrier (molecular weight of 154 Da) that is rapidly trapped and tightly bound in the thyroid cancer, or cleared from normal tissues and excreted in the urine, thereby providing a targeting index that can approach infinity. $^{131}$I-iodide commonly cures, otherwise incurable, metastatic thyroid cancer without significant toxicity (9). After one half century, $^{131}$I-iodide remains fundamental to imaging and therapy for metastatic thyroid cancer.

Lym-1 has been used as a carrier for several radioisotopes in imaging and therapy trials (10-13) because the basal level of HLA-DR expression on B lymphocytes is about 100 times lower than that found on malignant B lymphocytes (14,15) (Fig. 2). The Lym-1 Ab epitope is in the extracellular region of the beta subunit of human leukocyte antigen DR type (HLA-DR) 10, and related HLA-DRs. HLA-DR protein persists through B-cell differentiation, but disappears during transformation of the lymphocyte to the plasma cell stage (16). Early and pre-B lymphocytes are class 2 mRNA negative and cannot be induced to express class 2 proteins. HLA-DR protein is acquired during the late pre-B lymphocyte stage. HLA-DR is neither significantly shed nor internalized by lymphoma cells (17). Lym-1 Ab binding to lymphoma cells causes growth inhibition and apoptotic cell death (18-20).

The Lym-1 epitope is not shared by all HLA-DR subtypes (14,15). The critical Lym-1 binding residues are contained in the 19 differences in amino acid sequence between the reactive HLA-DR10 beta subunit and the unreactive, largely identical HLA-DR3 and HLA-DR52 beta subunits. Of the 19 residues comprising the critical Lym-1 binding region, only the amino acids Q70 or R70, followed by R71 were present in Lym-1 reactive and absent in Lym-1 unreactive NHL specimens. The hypothesis that the subtypes containing the putative critical Lym-1 binding residues (Q/R70-R71) would be most reactive was confirmed in a series of cytotoxicity assays conducted in lymphoblastoid cell lines of B and T cell type, incorporating 31 HLA-DR genotypes (15). Strongly reactive cells expressed at least one Q/R70-R71-containing HLA-DR allele while none of the least reactive cell lines expressed that sequence at position 70-71 of the beta subunit. Although Lym-1 reacted with peripheral blood lymphocytes from healthy donors, the avidities were much lower, consistent with a lower HLA-DR protein density on normal lymphocytes and the hypothesis that univalent rather than bivalent binding occurs. Thus, it seems that both the critical glutamine/arginine residues and a threshold antigen density contribute to the selectivity of Lym-1 binding to malignant over normal B-lymphocytes. Because the Lym-1 epitope on the beta subunit of HLA-DR10 was well characterized, it was selected for the design of Lym-1 Ab mimics to target radioisotopes to NHL for imaging and therapy.

First generation, bidentate SHALs discriminated HLA-DR10 expressing from non-expressing malignant cell lines (21), particularly in assay formats that involved avidins that increased affinity by effectively converting the bidentate SHALs to multivalent molecules. Although these bidentate SHALs bound selectively to HLA-DR10 expressing NHL cells *in vitro*, those tested have not shown anti-lymphoma activity (22), as does Lym-1 Ab (18-20). Experiments in mice with first generation, bidentate SHALs showed that individual ligands could unfavorably influence the tissue distribution of a SHAL (23). A bidentate SHAL that contained the ligands 4-dimethylaminoazobenzene-4'-sulfonyl-L-valine and N-alpha benzoyl-arginine-4-aminobenzoic acid, exhibited more desirable biodistribution. To increase SHAL residence time in the lymphoma, dimeric (bis) SHALs with different linker lengths between the constituent bidentate SHALs were generated by constructing two identical SHAL moieties from the alpha and epsilon amine of a lysine residue. Here, we characterize the behavior of several bis bidentate SHALs *in vitro* and *in vivo*.

## Materials and methods

*Antibodies and cell lines*. Murine (Peregrine Pharmaceuticals, Tustin, CA) and chimeric (provided by A. Epstein, Los Angeles, CA) Lym-1 Abs bind to an epitope on HLA-DR10 expressed on the surface of most NHL B-cells (16). Raji (American Type Culture Collection, Manassas, VA) and other lymphoma B-cells, B35M, Chevalier, Ramos, Raji clone 11, Granda, DG-75, SU-DHL-6, and NU-DHL-1 (provided by A. Epstein) were grown in RPMI-1640 with 10% fetal calf serum (FCS), supplemented with sodium pyruvate, non-essential amino acids (Gibco/Invitrogen, Carlsbad, CA), and antibiotics, at 37˚C in a humidified, 5% $CO_2$ atmosphere.

Malignant T-cells, CEM, and Jurkat's, breast cells, MCF7 and BT20, and prostate cells, LNCaP and DU145 were cultured as recommended, from American Type Culture Collection, Manassas, VA. Breast cancer cells, HBT-3477 (provided by Bristol-Myers Squibb, Seattle, WA) were cultured in Iscove's modified Dulbecco's medium with 15% FCS and the supplements identified above.

*Mouse model*. Female athymic Balb/c mice (Harlan, Frederick, MD), about 5 weeks old, were maintained according to University of California animal care guidelines, on a normal diet, *ad libitum*. The mice received 4 Gy (400 rads) external beam radiation 3 or 4 days before implantation to suppress immune response. Raji cells were harvested in logarithmic phase, centrifuged, and adjusted to $6x10^7$ cells/ml; 100 $\mu$l ($6x10^6$) of the cell suspension was injected subcutaneously into each side of the lower abdominal wall of each mouse. Studies for each SHAL were initiated about 3 weeks after implantation, when tumors were 50-500 mm$^3$. A total of 201 mice were studied; the number of mice for each SHAL ranged from 31 to 59.

*Study design*. Cell binding of biotin- and DOTA-SHALs were studied *in vitro*. Using $^{111}$In labeled DOTA-SHALs, pharmacokinetic investigations in mice at each of two different doses, about 1 (0.25 nM) and 20 (10 nM) $\mu$g, of 6 bis bidentate $^{111}$In-DOTA-SHALs ($(LeacPLD)_2LPDo$, $(ItPDP)_2LLDo$, $(DvLPBaPP)_2LLDo$, $(DvLPBaPPP)_2LLDo$, $(DvLPBaPPPP)_2$ LLDo, and $(DvLCsPBaPPP)_2CsLLDo$) included biodistribution, imaging, and WBAR. Mice were sacrificed 2, 4 and 24 h after injection of $^{111}$In-DOTA-SHAL for biodis-

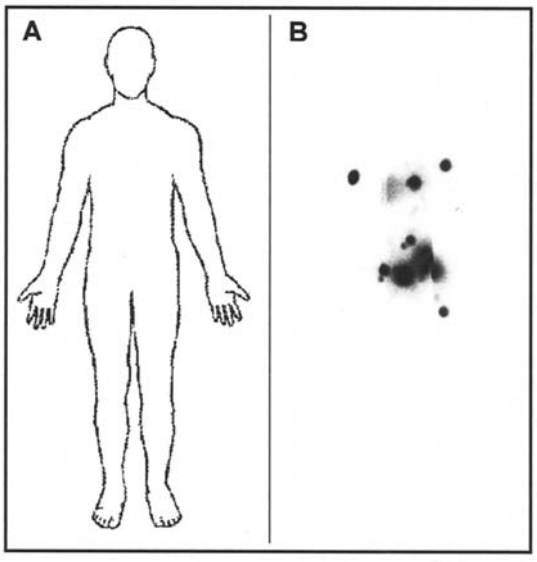


Figure 1. Whole body outline (A), and radioisotope image (B) of a patient with disseminated thyroid cancer (bone metastases) obtained 3 days after oral administration of $^{131}$I-iodide. $^{131}$I-iodide (sodium), having a molecular weight of 154 Da, was bound in the cancer or cleared in the urine, thereby providing a very high targeting index.

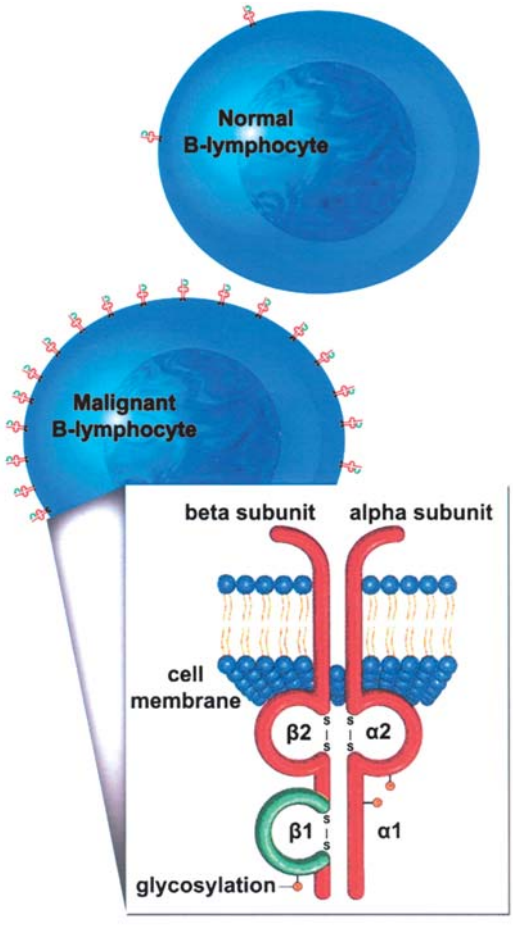


Figure 2. Schematic representation of the HLA-DR dimer. HLA-DR10 is a variant of the HLA-DR family of cell surface receptors found on normal B-cell lymphocytes and a variety of human lymphomas and leukemias. The beta subunit contains a unique epitope that is not present in the HLA-DR molecules found on other cells, and is expressed less, or not at all, on normal B-lymphocytes (modified from De Nardo, Biological Therapy of Lymphoma 2: 8, 1999).

tribution; 2 and 4 h after injection of $^{111}$In-DOTA-SHAL for WBAR; and mice were imaged 2, 4 and 24 h after injection of $^{111}$In-DOTA-SHAL. Blood samples were sequentially collected for $^{111}$In counting and selectively from some mice for serum assays.

*Cell binding*

*Cell binding to SA-HRP/SHAL coated wells*. One hundred $\mu$l of 25 $\mu$g/ml NeutrAvidin™ (Pierce, Rockford, IL) or streptavidin-horseradish peroxidase (SA-HRP; Invitrogen, Grand Island, NY) in PBS, 0.02% $NaN_3$, pH 7.2 were used to coat the wells of a Pro-bind (Falcon: Becton Dickinson, Franklin Lakes, NJ) plate, overnight at 4˚C. For positive control wells, Lym-1 at 1.0 $\mu$g/ml in PBS, 0.02% $NaN_3$, pH 7.2 was used. Excess coating solution was removed, wells washed three times with PBS and blocked for 2 h. One hundred $\mu$l of a 20-$\mu$M solution of the biotinylated SHALs (in 1% BSA/PBS) were added to the coated wells (100 $\mu$l of diluent was added to Lym-1 coated wells), and the plate was incubated for 1 h at room temperature, with rocking. Excess SHAL (or Lym-1) was rinsed from the plate by washing with 1% BSA/PBS three times, then 100 $\mu$l of 0.5x$10^7$ cells/ml in 5% BSA/PBS were added to wells and incubated at 37˚C for 1 hour. The wells were then rinsed twice with 1% BSA/PBS and twice with PBS. 100 $\mu$l of 10% buffered formalin was added to the wells for 10 min, removed, the wells rinsed 3x with PBS and bound cells were stained with 100 $\mu$l of filtered Crystal Violet stain (1% in water). After 10-20 sec, the plate was washed three times with 1X PBS to wash away excess dye. Plate wells were viewed by light microscopy at magnification x100-200 and photographed.

*ELISA using preincubated SHAL*. Biotinylated SHAL (10 $\mu$M) was incubated with 5 $\mu$g/ml SA-HRP in 1% bovine serum albumin solution in phosphate-buffered saline, pH 7.2 (BSA/PBS), for 1 h at room temperature. Cells were washed once and resuspended in 5% BSA/PBS to 10x$10^6$ cells/ml. One hundred $\mu$l of the SHAL solutions and 100 $\mu$l of the cell solutions were added to the wells of a 96-well plate, in triplicate, and incubated for 1 h at room temperature. Control wells contained diluent/SA-HRP in place of the SHAL/SA-HRP solution. After incubation, the cells were washed twice (BSA/PBS), centrifuged at 200 x g, and resuspended gently in 200 $\mu$l BSA/PBS. After the second wash, well contents were transferred to a new plate, washed once with BSA/PBS, and twice with PBS, in the manner described above. After centrifugation, 200 $\mu$l ABTS reagent (5 mM 2,2'-azino-bis-(3-ethylbenzthiazoline)-6-sulfonic acid in 50 mM citrate buffer, pH 4.2 with 0.3% $H_2O_2$) was added to the wells and color allowed to develop for 30 min. The plates were then centrifuged, 100 $\mu$l of the supernatant was removed to a new plate, and the absorbance at 405 nm was determined using a Dynatech MRX ELISA plate reader (Dynatech Laboratories Inc., Chantilly, VA). During the course of these binding studies, it was observed that the SHALs were not completely soluble at the higher concentrations used; this led to variability in the ELISA assay.

*Competitive binding assay*. To assess the functional affinity of $^{111}$In-DOTA-SHALs for Raji cells, which are HLA-DR10

positive, a competitive binding assay was performed using serially diluted SHAL, as previously described (22). Briefly, trace amounts (10 ng) of labeled SHAL [specific activity of 48.1 kBq/$\mu$g (1.3 $\mu$Ci/$\mu$g)] and varying amounts of SHAL were incubated with 1x10$^6$ cells in 5% BSA/PBS in a total volume of 150 $\mu$l for 1 h at ambient temperature. Cells were pelleted at 300 x g for 10 min and supernatant removed. Cell pellet and supernatant were counted in a calibrated gamma well counter (Pharmacia 1282 CompuGamma, Piscataway, NJ). The B/F was plotted against amounts of competitor to obtain binding affinity, using Scatchard analysis (24). The reported results are the averaged outcomes of experiments that involved replicate wells.

*Chemistry and radiochemistry*. Protein sequences for the crystal structures of four related HLA-DRs (1-4) were aligned and compared with the HLA-DR10 sequence to identify both the locations of the variable amino acids and those regions of HLA-DR10 containing amino acid residues identified as critical for the Lym-1 epitope. All five proteins exhibited a high degree of sequence similarity (93-96%) so that an accurate 3-D model of the HLA-DR10 beta subunit could be created using homology modeling. The coordinates of the model were used to screen for ligand binding with the program DOCK (25,26). Three sites were identified that surround the most important amino acid in the Lym-1 epitope, R70 (14,15).

Combinations of two ligands verified to bind to two of these sites within the Lym-1 epitopic region of HLA-DR were used to generate SHALs. The ligand combinations were deoxycholate (D) and leuenkephalin (Le), deoxycholate and triiodothyronine (It), deoxycholate and thyronine (T), and dabsylvaline (Dv) and N-Benzoyl-L-arginyl-4-aminobenzoic acid (Ba). A modular approach made it possible to synthesize for each ligand combination a series of SHALs containing different linker lengths, to switch out ligands with analogs or new ligands, and to create new SHALs with different pairs of ligands (Fig. 3). Briefly, SHALs were synthesized by connecting a site-1 ligand and a site-2 ligand using a lysine (L)/polyethylene glycol (PEG, P)-based linker and solid/polymer-supported synthesis on chlorotrityl chloride resin, as described in detail (27). All of the ligands used to generate the SHALs contained a carboxylic acid functional group for conjugation to the amino groups on lysine. The carboxyl group of the second lysine was linked to the alpha amino group of a primary lysine. The epsilon amino group of the primary lysine was used to attach a biotin or DOTA. The second lysine was used to link two SHALs together via the alpha and epsilon amines to produce a dimeric (bis) SHAL. Firstly, the carboxyl group of Fmoc-Lys(Boc)-OH was attached to chlorotrityl chloride resin and after Fmoc-deprotection, a second lysine, Dde-Lys(Fmoc)-OH was attached using standard amide coupling chemistry. The Boc-protecting group on the epsilon amine of the first lysine protected it throughout the solid phase synthesis. During cleavage of the SHALs from the polymer support, the epsilon amine on the first lysine was liberated and used to attach biotin, DOTA, or fluorescent dyes. Secondly, two equivalent branching motifs were constructed at the alpha and epsilon amine of the second lysine after Dde and Fmoc-deprotection. To study the effects of linker length on

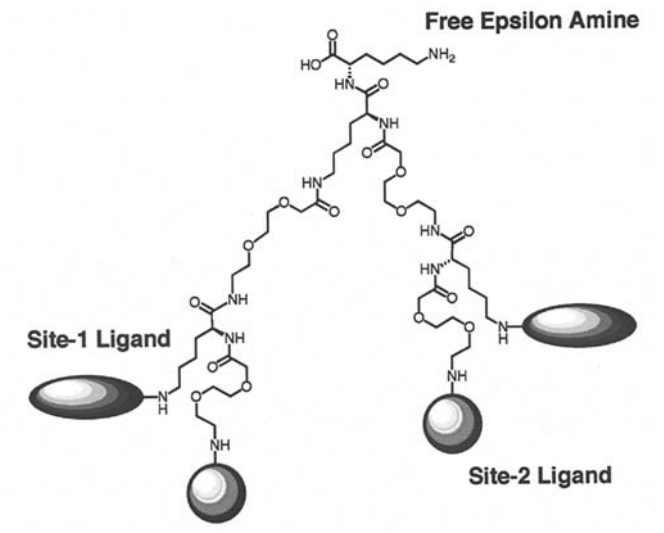


Figure 3. Schematic showing the modular, synthetic platform used to generate SHALs. Linkers comprised of lysine and PEG monomers are used to attach ligands in bidentate or bis bidentate SHALs. The length of the linkers can be easily altered by increasing or decreasing the number of PEG monomers. Additional ligands or functional components (e.g. internalizing peptides) can be incorporated at specific positions along the linker by inserting additional lysine residues. Tags (biotin, fluorescent dyes, $^{18}$F) or chelating groups (e.g. DOTA) can be added to facilitate assays and pharmacokinetic studies by attaching them to the third arm of the SHAL via the free epsilon amine of the primary lysine in the center of the linker.

binding affinity, one, two, or three PEG monomer spacers were built up via one, two, or three cycles of Fmoc-miniPEG-OH/Fmoc-deprotection. Next, the third lysine residues were inserted, again using Dde-Lys(Fmoc)-OH and followed with the construction of the bidentate SHAL motifs at the epsilon amine and at the alpha amine of the third lysine to produce a bis SHAL (27). Finally, the bis SHAL was cleaved from the polymer resin using 20% trifluoroacetic acid in dichloromethane and purified by reverse phase preparative HPLC. The SHALs were subsequently converted to biotin or DOTA SHALs by reacting with biotinyl-OSu and hexafluorophosphate salt of DOTA NHS ester respectively. For $(DvLCsPBaPPP)_2$ CsLLDo SHAL, cysteic acid residues were incorporated by sandwiching them between the lysine and PEG junctions, so that the polar sulfonic/sulfonate (SO3H/SO3-1) groups would improve the aqueous solubility of the SHAL.

The acronym for each SHAL is composed of a one or two letter code for the ligand, Lysine and PEG designated as L and P respectively, and DOTA and biotin designated as Do and B, respectively. The bis bidentate SHALs studied in mice and their corresponding acronyms are shown in Table I and Fig. 4. SHALs were purified using reverse phase high performance liquid chromatography (HPLC). Analytical HPLC was carried out at 1 ml/min on an Agilent 1100 instrument using a Waters Symmetry C18, 5 $\mu$m, 4.2x150 mm column and semi-preparative HPLC was carried out at 10 ml/min on a Waters Symmetryprep C18, 7 $\mu$m, 19x300 mm column. Both HPLC methods used a linear gradient from 95% $H_2O$ (1% TFA) to 80% MeCN (1% TFA) over 12 min and a diode array for detection. SHALs were characterized using proton and carbon NMR spectroscopy and electrospray mass spectro-

Table I. List of biotin and DOTA conjugated, bis bidentate SHALs tested.

| Acronym | Identity |
|---|---|
| Biotin-SHALs | |
| $(LeacPLD)_2LPB$ | bis-(acetylated 5-leuenkephalin PEG lysine deoxycholate) lysine PEG biotin |
| $(DvLPBaP)_2LLB$ | bis-(dabsyl-L-valine lysine PEG N-benzoyl-L-arginyl-4-aminobenzoic acid PEG) lysine lysine biotin |
| $(DvLPBaPPP)_2LLB$ | bis-(dabsyl-L-valine lysine PEG N-benzoyl-L-arginyl-4-aminobenzoic acid PEG PEG PEG) lysine lysine biotin |
| DOTA-SHALs | |
| $(LeacPLD)_2LPDo$ | bis-(acetylated 5-leuenkephalin PEG lysine deoxycholate) lysine PEG DOTA |
| $(ItPDP)_2LLDo$ | bis-(triiodothyronine PEG deoxycholate PEG) lysine lysine DOTA |
| $(DvLPBaPP)_2LLDo$ | bis-(dabsyl-L-valine lysine PEG N-benzoyl-L-arginyl-4-aminobenzoic acid PEG PEG) lysine lysine DOTA |
| $(DvLPBaPPP)_2LLDo$ | bis-(dabsyl-L-valine lysine PEG N-benzoyl-L-arginyl-4-aminobenzoic acid PEG PEG PEG) lysine lysine DOTA |
| $(DvLPBaPPPP)_2LLDo$ | bis-(dabsyl-L-valine lysine PEG N-benzoyl-L-arginyl-4-aminobenzoic acid PEG PEG PEG PEG) lysine lysine DOTA |
| $(DvLCsPBaPPP)_2CsLLDo$ | bis-(dabsyl-L-valine lysine cysteic acid PEG N-benzoyl-L-arginyl-4-aminobenzoic acid PEG PEG PEG) cysteic acid lysine lysine DOTA |

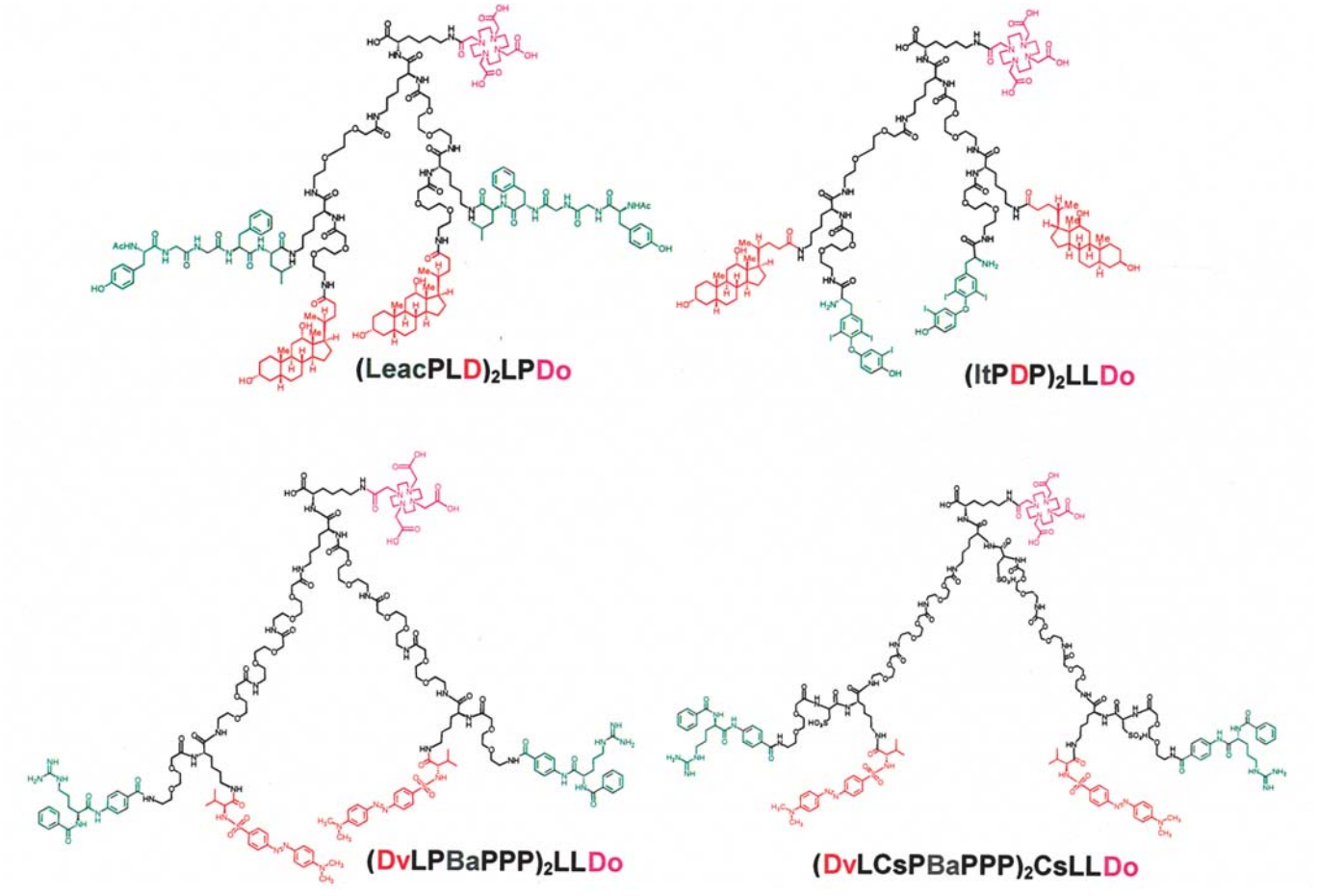


Figure 4. Bis bidentate SHAL chemical structures, and acronyms (in parentheses): $(LeacPLD)_2LPDo$, bis-(acetylated 5-leuenkephalin PEG lysine deoxycholate) lysine PEG DOTA; $(ItPDP)_2LLDo$, bis-(triiodothyronine PEG deoxycholate PEG) lysine lysine DOTA; $(DvLPBaPPP)_2LLDo$, bis-(dabsyl-L-valine lysine PEG N-benzoyl-L-arginyl-4-aminobenzoic acid PEG PEG PEG) lysine lysine DOTA; $(DvLCsPBaPPP)_2CsLLDo$, bis-(dabsyl-L-valine lysine cysteic acid PEG N-benzoyl-L-arginyl-4-aminobenzoic acid PEG PEG PEG) cysteic acid lysine lysine DOTA. $(DvLPBaPP)_2LLDo$, bis-(dabsyl-L-valine lysine PEG N-benzoyl-L-arginyl-4-aminobenzoic acid PEG PEG) lysine lysine DOTA and $(DvLPBaPPPP)_2LLDo$, bis-(dabsyl-L-valine lysine PEG N-benzoyl-L-arginyl-4-aminobenzoic acid PEG PEG PEG PEG) lysine lysine DOTA were also studied in mice.

metry. All SHALs were found to have molecular weights within 0.07% of their theoretical molecular weight.

DOTA-SHAL radiochemistry has been previously described in detail (23,27). Briefly, DOTA-SHALs were labeled with $^{111}InCl_3$ in 0.05 M HCl (MDS Nordion, Vancouver, Canada); an aliquot of $^{111}InCl_3$ (148-185 MBq, 4-5 mCi, 15-20 $\mu$l) was added to a solution of DOTA-SHAL (25-50 $\mu$g) 10% DMSO in 0.1 M $NH_4OAc$ (50 $\mu$l) and the pH of the reaction mixture adjusted to 6-7 by adding 4 M $NH_4OAc$. The reaction mix was incubated for 1 h at 37˚C, then 0.1 M EDTA (10-20 $\mu$l) was added to sequester free $^{111}In^{3+}$. The reaction mixture was purified using RP-HPLC (Beckman Coulter System Gold 128 with radioactive detector, Raytest USA, Wilmington, NC) at 1 ml/min (C-18 column, linear gradient of 1% TFA in $H_2O$ 95% to 1% TFA in $CH_3CN$ 90% >15 min) $^{111}$In-DOTA-SHALs eluted between 9-12 min. The purified $^{111}$In-DOTA-SHALs were concentrated using a Speedvac SC110 (Savant Instruments, Holbrook, NJ) and the products redissolved in 10% DMSO in PBS. Quality assurance was determined using C-18 thin layer chromatography (TLC), high performance liquid chromatography (HPLC), and cellulose acetate electrophoresis (CAE). TLC, HPLC, and CAE showed distinct peak resolution between $^{111}$In-DOTA-SHAL and $^{111}$In-EDTA. $^{111}$In-DOTA-SHAL product yields ranged from 70 to 90% and the purity of the product ranged from 90 to 95%. The $^{111}$In-DOTA-SHALs were stable up to 72 h at room temperature.

*Pharmacokinetics*

*Biodistribution*. $^{111}$In-DOTA-SHAL (100 $\mu$l) was injected into the tail vein of each mouse. The injected radioactive dose was measured by counting the mouse immediately after injection, using two opposed, isoresponsive sodium iodide detectors (Canberra Nuclear, Meriden, CT). To determine total body clearances, mice were counted immediately and serially for 24 h after injection using the isoresponsive sodium iodide detector system; the counts were decay corrected and expressed as % ID. Blood clearances were determined by collecting blood samples (2 $\mu$l) over 24 h from the dorsal tail vein and counting them in a sodium iodide gamma well counter (Wallac LKB, Turku, Finland). Decay-corrected radioactivity in the blood was expressed as % ID, using a weight-based theoretical blood volume. Pharmacokinetic data for other tissues were obtained by sacrificing mice at 2, 4, and 24 h after injection, removing and weighing the tissues, and counting them in the same gamma well counter. The concentration of radioactivity in each organ was expressed as % ID/g.

*Whole body autoradiography (WBAR)*. WBAR studies were conducted as previously described (28,29); each mouse was anesthetized with 5 mg/100 $\mu$l aqueous solution of sodium pentobarbital i.p., flash frozen in a hexane-dry ice bath, and embedded in frozen 4% carboxymethylcellulose. Sagittal sections of 50 $\mu$m thickness taken to show tumors, spleen, kidney, liver and the midline of the vertebral column were taken at -20˚C with a cryomicrotome (Leica Polycut, Nussloch, Germany). The sections then were desiccated, and autoradiograms were prepared by exposing the sections to X-ray film (Kodak BioMax MS, Rochester, NY).

*Plasma/serum transport/stability*

Human plasma stability studies *in vitro*. Human plasma (Sacramento Blood Bank, lot #FJ62337), stored at -80˚C, was thawed and sterile filtered just prior to the addition of radiolabeled $^{111}$In-DOTA-SHAL, 0.7-4.3 $\mu$g/ml. The SHAL-plasma mixture, and plasma alone, was incubated at 37˚C in a 5% $CO_2$ atmosphere. Aliquots taken periodically for 7 days were analyzed using cellulose acetate electrophoresis (CAE) for 45 min at 300 V in Tris-barbital-sodium buffer, pH 8.6 (DiaSys Europe, Ltd., Wokingham, Berkshire, UK). Strips containing the SHAL-plasma mixture were imaged on a phosphor imager (Fuji BAS1800II, Kanagawa, Japan), and strips containing plasma alone were fixed in 20% sulfosalicilic acid, rinsed in $H_2O$, stained with 0.25% Coomassie blue in water and destained with 30% methanol and 10% acetic acid. The electromobility of the SHAL was compared to that of the known plasma proteins.

Mouse serum studies *in vivo*. Mice were euthanized 2 and 4 h after injection of radiolabeled SHAL and exsanguinated by cardiac puncture. The blood was allowed to clot and was centrifuged at 11,000 x g for 5 min and the serum was separated. Serum samples were electrophoresed as described above for comparison to the radiochemical alone and in human plasma. Samples with sufficient activity were also chromatographed (HPLC) using molecular weight sieving SEC3000 columns at 1 ml/min in 0.1 M sodium phosphate buffer, pH 7.1 in order to estimate the molecular weights of the circulating SHAL.

Immunoprecipitation studies. Human plasma (20 $\mu$l) aliquots were mixed with goat anti-human transferrin, goat anti-human albumin, goat anti-human IgG, or goat anti-human ceruloplasmin (Sigma, St. Louis, MO) in excess amounts to precipitate these proteins, held for 1 h at room temperature, then centrifuged at 12,000 x g for 10 min. The supernatants and precipitates were carefully separated and the activity of each measured by counting in a gamma well counter. The activity in the precipitate was expressed as a percent of the total activity.

*Statistical analysis*. Data is reported as the mean ± SD. Statistical comparisons were based on the Wilcoxon rank sum test (30), a procedure based on ranking the values of two test groups. Differences were considered statistically significant at p-values $\leq$0.05. Clearances were assessed using least-mean-square linear regression analyses of % ID vs time for monoexponential and biexponential fits. The p-values were estimated assuming a normal distribution of data about the mean determined by a Z transformation of the correlation coefficient (31). Additionally, monoexponential fits for all mice in a group and only the mice followed for 24 h were compared and found to be insignificantly different.

## Results

*SHAL chemistry*. Biotinylated and DOTA-tagged bis bidentate SHALs were synthesized in multimilligram amounts at high purity; DOTA-SHALs were labeled with $^{111}$In at high efficiency, specific activity, and purity. Median radiochemical labeling and final product yields were 95% (range: 50-95%) and 90% (range: 45-92%), respectively; specific activities

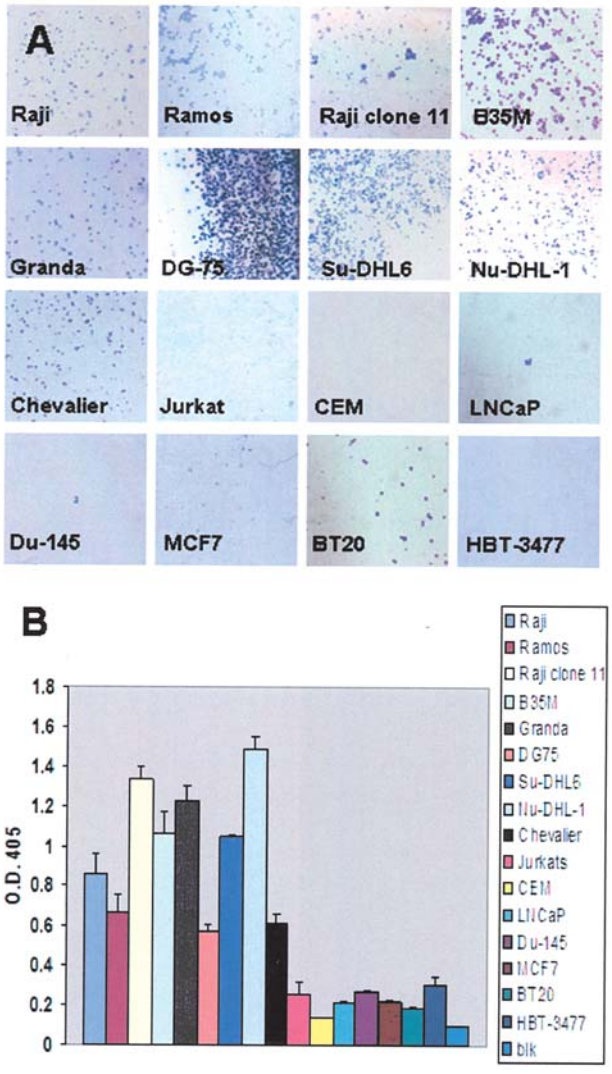


Figure 5. SHAL binding to live cells. A, Results of cell-binding assay for 9 HLA-DR10 expressing B-lymphoma cell lines (top 2 rows and Chevalier), and HLA-DR10 negative malignant cell lines, T-lymphoma (Jurkat's, CEM), prostate cancer (LNCaP, Du-145), and breast cancer (MCF7, BT20, HBT-3477). Cells were incubated in wells coated with neutravidin and biotinylated-$(DvLBaPPP)_2$LLB. Only cells expressing HLA-DR10 bound to the wells. B, ELISA with the same cell lines. Cells were incubated with biotinylated-SHAL (pre-incubated with SA-HRP) and washed thoroughly. HRP substrate was added, cells were pelleted by centrifugation, and the supernatant absorbance at 405 nM was measured. Cells positive for HLA-DR bound more of the SHAL/SA-HRP complex, giving a higher signal. The nine B-lymphoma cell lines are on the left.

were 3.8 MBq/$\mu$g, range: 3.0-4.0 MBq/$\mu$g (102 $\mu$Ci/$\mu$g, range: 82-110 $\mu$Ci/$\mu$g), and 13.2 MBq/nM, range: 10.3-13.5 MBq/nM (358 $\mu$Ci/nM, range: 279-365 $\mu$Ci/nM). $^{111}$In-DOTA-SHAL products were 90% pure (range: 85-97%).

*Cell binding*. HLA-DR10 positive lymphoma cells bound to coated wells to which SHALs (Fig. 5) or Lym-1 Ab (not shown) was added. Malignant cells (T-cell lymphoma, breast cancer, prostate cancer) that do not express HLA-DR10 did not bind to the wells. Binding to uncoated, blocked wells was minimal for all cell lines. Additionally, live cell ELISAs indicated that SHAL binding to cells was typically higher for cell lines that express HLA-DR10.

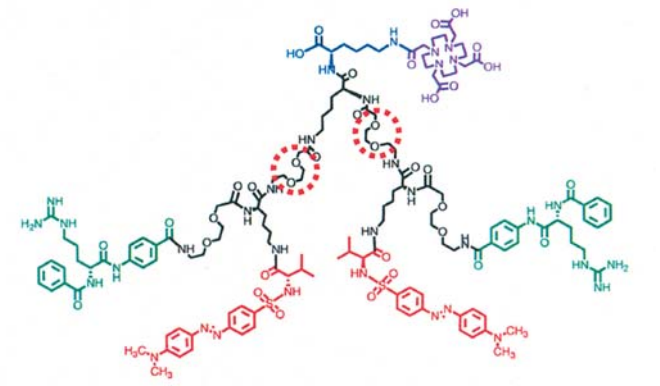

Figure 6. Relationship between the number of PEG monomers (interrupted circles) in each linker of the bis bidentate SHAL, $(DvLPBaPP)_2$LLDo. The estimated span in Angstroms (Å), assuming linearity, for 4, 6, and 8 PEG monomers are 53, 75, and 97 Å, respectively.

The affinity of the bis SHALs increased when the length of the linker was increased above about 50 Å. For the bis bidentate SHAL $(DvLPBa[P]_n)_2$LLDo, in which the linker contained 2-8 PEG monomers (Fig. 6), in addition to the lysine to which the DOTA was attached, the functional affinity of the SHALs increased from $10^{-8}$-$10^{-9}$ (near nanomolar) to $10^{-9}$-$10^{-10}$. However, the body and blood clearances of the $(DvLPBa[P]_n)_2$LLDo SHALs remained similar (Fig. 7).

*Pharmacokinetics*. No toxicity was observed in the mice after injection of the SHALs. For each SHAL, the pharmacokinetics of the $^{111}$In-labeled SHAL was studied in mice by measuring the biodistribution of the SHAL and its clearance time in 16 tissues. For practical reasons, data are shown for a subset of the tissues (Fig. 8). The pharmacokinetics did not vary with the administered mass of the SHAL (Figs. 7-9). Both body and blood clearances of the bis bidentate SHALs in the xenografted mice were best fit with a monoexponential function. Blood clearance half-times varied between 3.6 and 9.5 h, whereas body clearance half-times varied between 15.2 and 43.0 h (Table II and Fig. 7). In the mice, SHALs containing peptide ligands were directed to the kidney (Figs. 8 and 9). Others containing deoxycholate showed that this bile acid-like ligand resulted in substantial uptake by the liver. $(LeacPLD)_2$PDo showed biliary processing; $(ItPLD)_2$LLDo containing deoxycholate and triiodothyronine ligands showed liver uptake and bound to prealbumin receptor (see Plasma Transport). Biodistribution, WBAR and radioisotope imaging revealed modest uptake of the bis SHALs in HLA-DR10 expressing Raji xenografts (Figs. 8-10). If the bis SHALs were directed to specific organs by a particular ligand, they accumulated to a higher level in the tissue than the corresponding bidentate SHAL, perhaps because the ligand was duplicated in the bis version. For example, the concentration in the liver of bis SHAL, $(ItPDP)_2$LLDo, containing two deoxycholate ligands was ~50% ID/g over 24 h (compared to ~20%ID/g for the analogous bidentate SHAL, ItPLDDo; data not shown). To increase SHAL solubility and at the same time provide other functional groups on the linker that might bind to the arginine residue located between the two cavities that form the SHAL binding

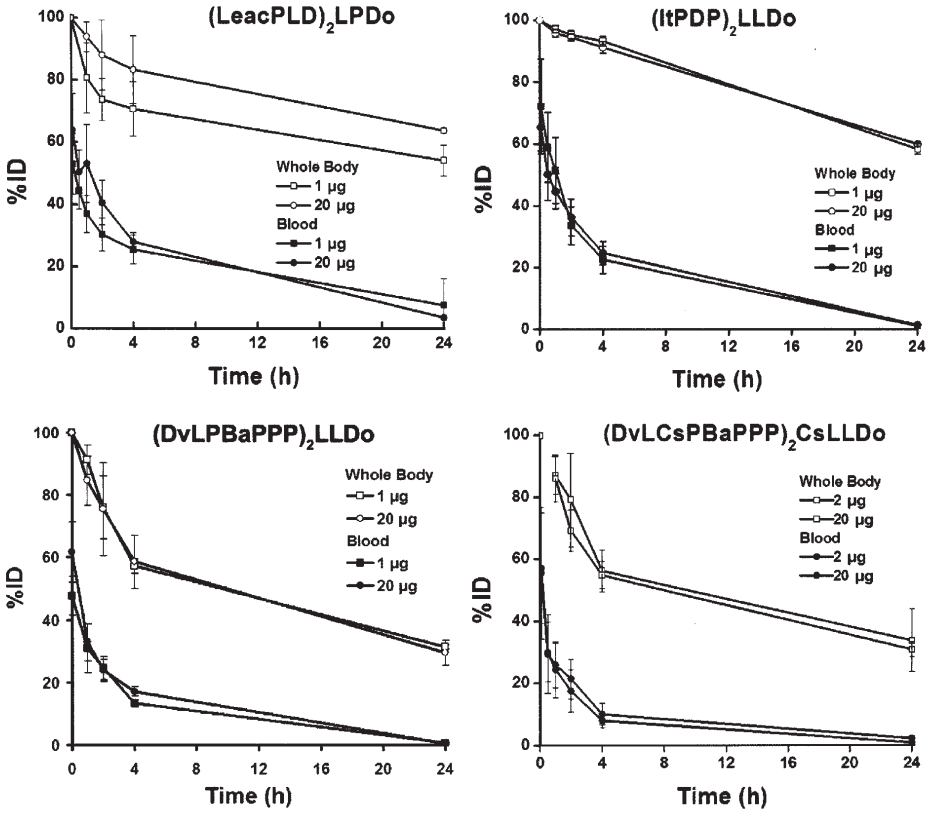


Figure 7. Whole body and blood clearances of bis bidentate SHALs ($(LeacPLD)_2LPDo$, $(ItPDP)_2LLDo$, $(DvLPBaPPP)_2LLDo$), and $(DvLCsPBaPPP)_2CsLLDo$ in mice. Clearances were similar whether 1 or 20 $\mu$g of SHAL was given intravenously. Additionally, the blood and body clearances of $(DvLPBa[P]_n)_2LLDo$ were similar (see Results for details).

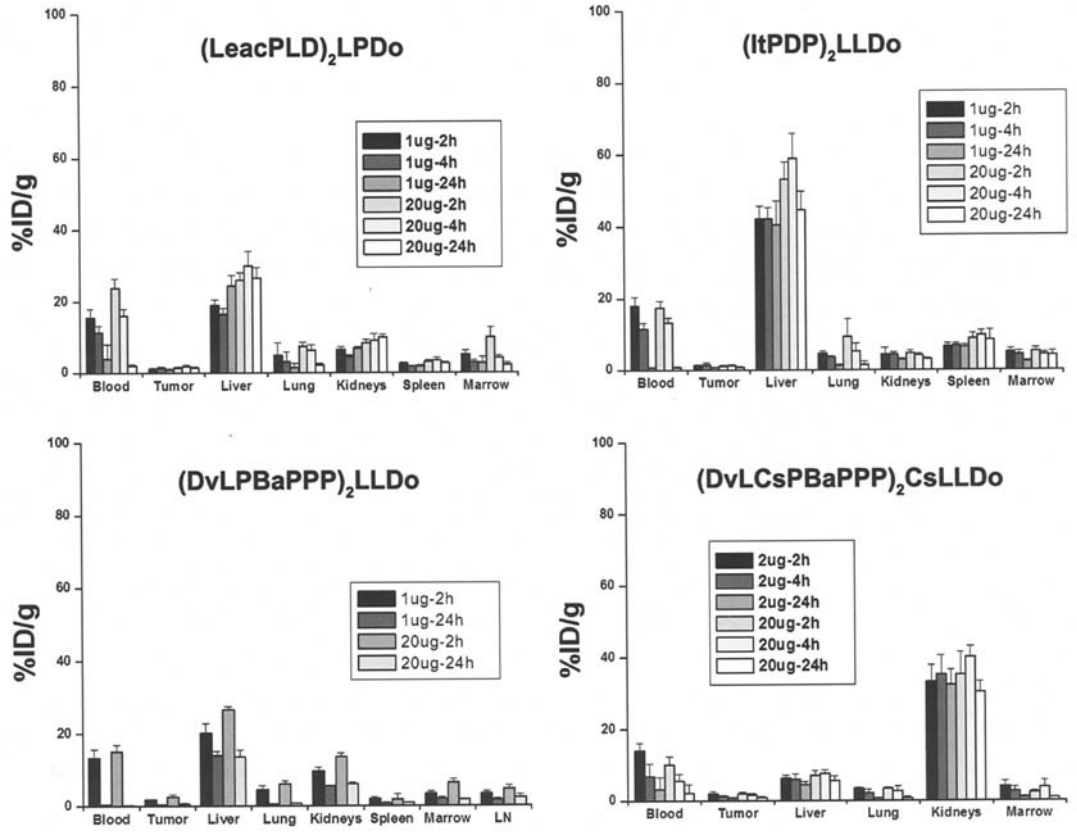


Figure 8. Tissue pharmacokinetics for bis bidentate SHALs in mice. Pharmacokinetics revealed liver and kidney localization, probably determined by the ligands leuenkephalin and deoxycholate, the rapid clearance of the bis bidentate SHAL in which the linker was too short to permit bivalent binding, and no mass effect. SHAL, $(DvLPBaPPP)_2LLDo$, in which dabsylvaline and aminobenzoic acid replaced the peptides and deoxycholate, did not accumulate in normal tissues.

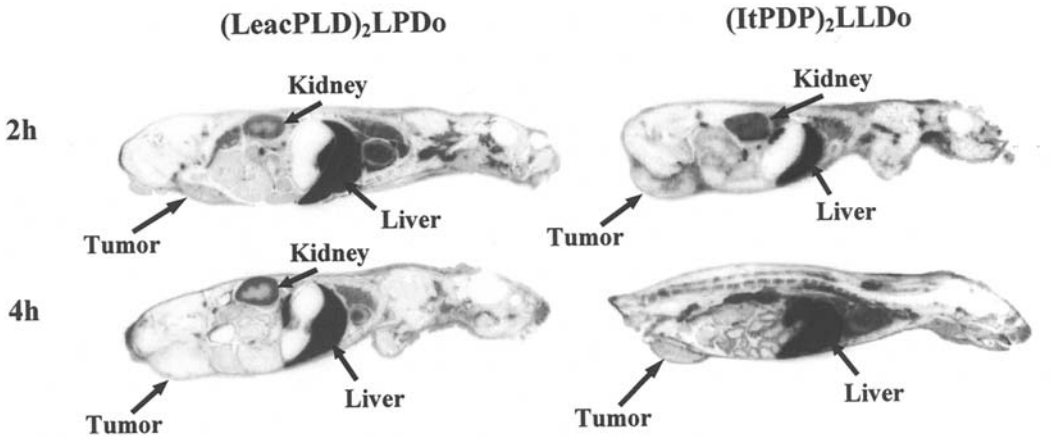


Figure 9. WBARs of mice euthanized 2 (upper) and 4 (lower) hours after i.v. injection of 20 $\mu$g of $^{111}$In radiolabeled bis bidentate forms of deoxycholate-leuenkephalin and deoxycholate-triiodothyronine SHALs. These SHALs showed kidney and liver localization, respectively, and activity in the intestinal contents.

Table II. Blood and whole body clearances for each of the SHALs given to mice i.v. in 1 or 20 $\mu$g (p-value).

| SHAL | Blood half-times (hours) 1 $\mu$g (p-value) | | 20 $\mu$g (p-value) | |
|---|---|---|---|---|
| $(LeacPLD)_2LPDo$ | 9.5 | (0.02) | 6.0 | (0.01) |
| $(ItPDP)_2LLDo$ | 4.1 | (<0.01) | 4.5 | (<0.01) |
| $(DvLPBaPP)_2LLDo$ | 4.0 | (<0.01) | 3.9 | (<0.01) |
| $(DvLPBaPPP)_2LLDo$ | 4.3 | (0.01) | 3.6 | (0.01) |
| $(DvLPBaPPPP)_2LLDo$ | 3.7 | (0.01) | 3.6 | (0.01) |
| $(DvLCsPBaPPP)_2CsLLDo$ | 6.1 | (0.04) | 4.2 | (0.02) |
| | Whole body half-times (hours) 1 $\mu$g (p-value) | | 20 $\mu$g (p-value) | |
| $(LeacPLD)_2LPDo$ | 37.6 | (0.09) | 43.0 | (0.02) |
| $(ItPDP)_2LLDo$ | 30.8 | (<0.01) | 33.2 | (<0.01) |
| $(DvLPBaPP)_2LLDo$ | 18.7 | (0.01) | 22.1 | (0.01) |
| $(DvLPBaPPP)_2LLDo$ | 15.8 | (0.03) | 15.2 | (0.02) |
| $(DvLPBaPPPP)_2LLDo$ | 16.4 | (0.04) | 15.6 | (0.04) |
| $(DvLCsPBaPPP)_2CsLLDo$ | 23.6 | (0.04) | 21.5 | (0.04) |

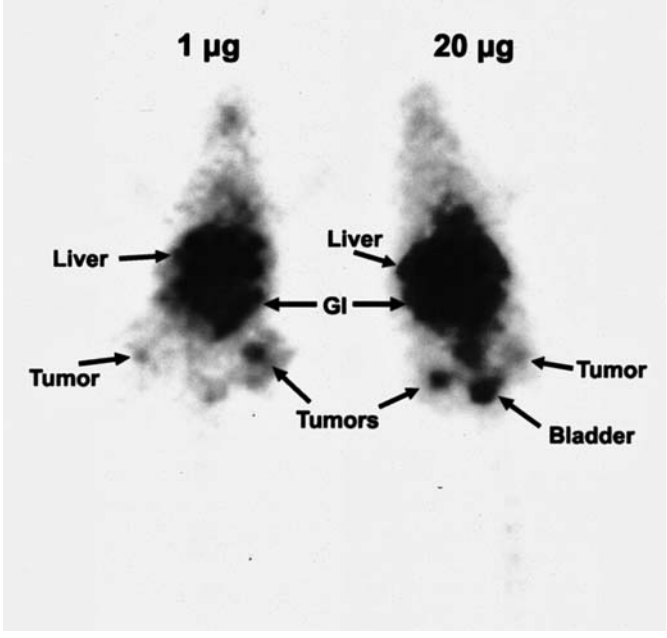


Figure 10. To assess SHAL potential for molecular imaging and therapy, radioisotope images of two pronely positioned Balb/c nu/nu mice were obtained 4 h after i.v. $^{111}$In-$(LeacPLD)_2LPDo$ (7.4 MBq, 200 $\mu$Ci; 1 or 20 $\mu$g). Each mouse has subcutaneous Raji HLA-DR10 expressing xenografts on the lower abdomen, right and left sides. Uptake is observed in these xenografts and in the liver and gastrointestinal tract (GI).

site, cysteic acid was added to the linker of the bis SHAL $(DvLCsPBaPPP)_2CsLLDo$. Solubility was improved, but addition the of cysteic acid led to an increase in SHAL accumulation in the kidneys (Fig. 8).

*Plasma/serum transport/stability*. The electrophoretic and molecular sieving chromatographic behavior of the DOTA-SHALs remained constant in human plasma over seven days and in mouse serum *in vivo* over 24 h. As an additional indicator of SHAL stability, immunoprecipitation studies showed no radioactivity bound to IgG, albumin, transfererrin, or ceruloplasmin. Whether in the absence or presence of human plasma or mouse serum, all but one SHAL, $(ItPLD)_2LLDo$, electrophoresed at or near the origin and eluted from a molecular sieving column near the column volume, showing that the DOTA-SHALs were nearly neutral and less than 5 kDa in size. $(ItPLD)_2LLDo$, a SHAL containing triiodothyronine and deoxycholate ligands, bound to prealbumin, a thyroid hormone receptor. This SHAL remained at the origin on electrophoresis unless human plasma was added. In human plasma at 1.4 $\mu$g/ml, 50% of the activity migrated at 1.9 cm, and 50% migrated at 2.9 cm; this pattern was stable over 5 days. At a plasma concentration of 4.3 $\mu$g/ml, 53% of the SHAL activity remained at the origin, 25% migrated 1.9 cm, and

23% migrated 2.9 cm. In the presence of mouse serum, 50% migrated 3.7 cm and 50% remained at the origin. Sera collected from mice 2 and 4 h after SHAL injection showed all of the activity migrating at 3.7 with prealbumin.

## Discussion

A series of SHALs have been synthesized based on the knowledge that the affinity of small ligands can be dramatically increased by combining them (6,32,33). Using computer modeling and experimental binding studies, ligands were selected because of their affinity for sites within the Lym-1 epitopic region of HLA-DR protein and chemistry favorable for attachment to a linker comprised of lysine and PEG monomers. First generation bidentate SHALs showed the desired selectivity *in vitro* and many of the intended pharmacokinetic characteristics in mice (21,23). One of the SHALs has been shown to bind to human lymphoma cells with a pattern of binding that mimicked that of the Lym-1 antibody (21). Dimeric (bis) bidentate SHALs (<5 kDa) were subsequently synthesized using a similar lysine-PEG platform. Although both bidentate and bis bidentate SHALs were selective for HLA-DR expressing cells in assays, the length of the linker used to create the initial bis SHALs was short (a single lysine and PEG monomer); these bis SHALs bound to Raji cells with an affinity similar to that of the bidentate SHALs. Three bis bidentate versions of DvLPBaPLDo SHAL, ((DvLPBaPP)$_2$LLDo, (DvLPBaPPP)$_2$LLDo, and (DvLPBaPPPP)$_2$LLDo) were synthesized with linkers spanning 50-90 Å (linker lengths calculated based on the assumption that the PEG units are fully extended). These bis bidentate SHALs exhibited higher functional affinities for Raji cells, suggesting that longer linkers may allow binding to two neighboring HLA-DRs on the cell surface. These behavioral relationships are analogous to the relationship of a single chain variable fragment to its parent Ab.

Following analyses of binding *in vitro*, the tissue distribution and kinetics of the bis bidentate SHALs were assessed in mice using DOTA-SHALs labeled with $^{111}$In at high specific activity and purity. SHAL selectivity *in vivo* depends on the assumption that binding of the individual ligands of the SHAL to non-target proteins is weak and the off-rate is fast, so that non-specific binding contributed by individual ligands is minimal. This underlying concept needs to be modified based on the observations in mice that, under some circumstances, ligands can influence SHAL behavior. Bis bidentate SHALs containing deoxycholate ligands localized in the liver of the mice. SHALs containing peptide-like ligands accumulated in the kidneys, while those containing the triiodothyronine ligand, a thyroid hormone, bound to high affinity proteins in the blood. In retrospect, some of these problems were predictable, and have been subsequently addressed by better ligand selection. Better ligand selection led to a SHAL ((DvLPBaPPP)$_2$LLDo) that rapidly cleared from normal tissues. Replacing deoxycholate with dabsylvaline and leuenkephalin or triiodothyronine with benzoyl-L-arginyl-4-aminobenzoic acid eliminated normal tissue localization. Replacement of peptide or peptide-like ligands eliminated plasma binding and kidney uptake. Changes in these bis bidentate SHALs can be made to improve their effectiveness for molecular imaging and therapy. Despite only modest NHL tumor uptake *in vivo*, the kinetics of the bis bidentate SHALs suggest potential for imaging NHL (Fig. 10). However, clearances of tumor bound SHALs were rapid, indicating that the off-rate needs to be reduced to improve their potential for therapy. The modular platform used to create the SHALs facilitates the introduction of different ligands, linkers, and other components (e.g., biotin, radioisotopes, fluorescent dyes, internalizing peptides, etc) while preserving the ability to rapidly produce large amounts of highly pure SHALs (Fig. 3). Ligands containing free carboxyl or amino groups are attached to the two ends of a linker created, using a combination of lysine residues and PEG monomers. The distance between ligands or SHALs can be increased or decreased simply by increasing or decreasing the number of PEG monomers. Sites for attaching additional ligands or functional moieties can be created by incorporating additional lysine residues at appropriate positions within the linker. The amide coupling chemistry used to combine linker components and attach ligands is performed under mild conditions, and it is inexpensive, rapid, and efficient. The same approach used to create bidentate SHALs containing two ligands was also used to produce multimeric SHALs. Once a successful SHAL is identified, gram amounts can be synthesized for a fraction of the cost of biologic-based therapeutics. By replacing biotin with DOTA, SHALs provide a chelator suitable for a variety of metals and lanthanides (34) for magnetic resonance imaging, nuclear imaging, positron imaging, and therapy. The lysines in the linkers provide sites for halogenation (35). $^{131}$I, a radioisotope suitable for imaging and therapy, or $^{18}$F, a positron emitter for PET imaging can be covalently linked. Additionally, the linker can be used to attach internalizing peptides (36) that facilitate transport of the SHAL and associated radiometals or other tags into cells.

We have begun to apply new approaches for modifying existing SHALs, and creating new ones, that will be retained better by lymphoma tissue. Because the dabsylvaline and N-benzoyl-L-arginyl-4-aminobenzoic acid ligand combinations showed the required selectivity, new dabsylvaline and N-benzoyl-L-arginyl-4-aminobenzoic SHAL derivatives have been synthesized. A modified form of the dabsylvaline and N-benzoyl-L-arginyl-4-aminobenzoic acid SHAL that contained a cysteic acid residue at the junction of the two ligand-containing arms of the SHAL was created as the first of a series of SHALs containing reactive functional groups that bind electrostatically or covalently to neighboring amino acid side chains on the beta subunit. In this case, the cysteic acid was positioned in the sequence such that it could form a salt bridge with Arg70 when the SHAL binds to HLA-DR10. This SHAL was more soluble, but did not show improved performance *in vivo*. SHAL affinity and selectivity can be further improved by incorporating additional ligands designed to bind to other sites either within or external to the Lym-1 epitopic region. Additional computational analyses of the modeled structure of the HLA-DR10 beta subunit have led to the identification of several new binding sites, and sets of ligands for these sites, that can serve for creation of tridentate or alternate bidentate SHALs.

Other approaches include modifications that facilitate SHAL internalization into the cell to direct 'residualizing'

metals, thereby increasing lymphoma residence time. Several groups have demonstrated that short polypeptide sequences attached to proteins induce their transport/internalization into cells to which the molecules bind (37-40). Based on work by others that the hexa-arginine sequence facilitates internalization into cells (39,40), a modified form of the SHAL ($(DvLPBaPPP)_2$ LL-$(arg)_6$), containing the D-isomeric form of arginine $(arg)_6$ to minimize proteolytic degradation *in vivo*, attached to a third arm on the linker is planned.

In addition to using modular synthetic chemistry, SHALs can also be created using bead-based combinatorial chemistry (41,42). A highly focused library can be synthesized on the beads, added to HLA-DR expressing cells, allowed to bind, and washed to remove unbound or weakly bound beads. Bead binding can then be assessed by examining the cells under a microscope.

Artificially reducing the molecular weight of a drug provides a means to increase the amount of drug going to the tumor while reducing toxicity to the rest of the body. However, the stay of chemotherapeutic drugs inside tumors is brief because they flow out as rapidly as they enter. Because our goal was to increase the tumor dose and lower the normal tissue dose, a series of novel drugs, SHALs, were synthesized for targeted delivery against membrane antigens preferentially expressed on lymphoma cells. The characteristics of these new molecules illustrate the importance of ligand selection and linker technology for developing drugs for cancer imaging and therapy. The results presented here demonstrate that it is possible to create molecular-based targeting drugs with an overall molecular weight less than 5 kDa that exhibit high affinity and selectivity for their target protein, can be labeled in high yield and may prove useful as alternatives to traditional Ab-based targeting systems. SHALs have a shelve life measured in years, and an availability and cost preferable to those of biologically-generated material. This technology established to target HLA-DR can be transferred to other protein targets of relevance.

## Acknowledgements

This study was supported by National Cancer Institute PO1-CA47829 and Lawrence Livermore National Laboratory LDRD Awards 01-ERD-111, 01-ERD-046, and 01-SI-012, under the auspices of USDOE contract W-7405-ENG-48. We thank Laird Miers, Cheng-Yi Xiong, and Elaine Hoye for assistance in data assembly and manuscript preparation.

## References

1. McLaughlin P, Grillo-Lopez AJ, Link BK, Levy R, Czuczman MS, Williams ME, Heyman MR, Bence-Bruckler I, White CA, Cabanillas F, Jain V, Ho AD, Lister J, Wey K, Shen D and Dallaire BK: Rituximab chimeric anti-CD20 monoclonal antibody therapy for relapsed indolent lymphoma: half of patients respond to a four-dose treatment program. J Clin Oncol 16: 2825-2833, 1998.
2. Witzig TE, White CA, Wiseman GA, Gordon LI, Emmanouilides C, Raubitschek A, *et al*: Phase I/II trial of IDEC-Y2B8 radioimmunotherapy for treatment of relapsed or refractory $CD20^+$ B-cell non-Hodgkin's lymphoma. J Clin Oncol 17: 3793-3803, 1999.
3. DeNardo GL, Sysko VV and DeNardo SJ: Cure of incurable lymphoma. Int J Radiat Oncol Biol Phys 66: S46-S56, 2006.
4. Press OW, Eary JF, Appelbaum FR, Martin PJ, Badger CC, Nelp WB, Glenn S, Botchko G, Fisher D, Porter B, Matthews DC, Fisher LD and Bernstein ID: Radiolabeled-antibody therapy of B cell lymphoma with autologous bone marrow support. N Engl J Med 329: 1219-1224, 1993.
5. Mammen M, Choi S and Whitesides GM: Polyvalent interactions in biological systems: implications for design and use of multivalent ligands and inhibitors. Agnew Chem Int Edit 37: 2755-2794, 1998.
6. Kramer RH and Karpen JW: Spanning binding sites on allosteric proteins with polymer-linked ligand dimers. Nature 395: 710-713, 1998.
7. Hajduk PJ, Meadows RP and Fesik SW: Discovering high-affinity ligands for proteins. Science 278: 497-499, 1997.
8. Fan E, Merritt EA, Verlinde CL and Hold WG: AB(5) toxins: structures and inhibitor design. Curr Opin Struct Biol 10: 680-686, 2000.
9. Mazzaferri EL and Jhiang SM: Long-term impact of initial surgical and medical therapy on papillary and follicular thyroid cancer. Am J Med 97: 418-428, 1994.
10. DeNardo GL, DeNardo SJ, O'Grady LF, Levy NB, Adams GP and Mills SL: Fractionated radioimmunotherapy of B-cell malignancies with $^{131}$I-Lym-1. Cancer Res 50 (Suppl.): 1014-1016, 1990.
11. DeNardo GL, De Nardo SJ, Kukis DL, O'Donnell RT, Shen S, Goldstein DS, Kroger LA, Salako Q, DeNardo DA, Mirick GR, Mausner LF, Srivastava SC and Meares CF: Maximum tolerated dose of $^{67}$Cu-2IT-BAT-Lym-1 for fractionated radioimmunotherapy of non-Hodgkin's lymphoma: a pilot study. Anticancer Res 18: 2779-2788, 1998.
12. DeNardo GL, DeNardo SJ, O'Donnell RT, Kroger LA, Kukis DL, Meares CF, Goldstein DS and Shen S: Are radio-metal-labeled antibodies better than Iodine-131-labeled antibodies: comparative pharmacokinetics and dosimetry of copper-67-, iodine-131-, and yttrium-90-labeled Lym-1 antibody in patients with non-Hogkin's lymphoma. Clin Lymphoma 1: 118-126, 2000.
13. DeNardo GL, O'Donnell RT, Shen S, Kroger LA, Yuan A, Meares CF, Kukis DL and DeNardo SJ: Radiation dosimetry for $^{90}$Y-2IT-BAD-Lym-1 extrapolated from pharmacokinetics using $^{111}$In-2IT-BAD-Lym-1 in patients with non-Hodgkin's lymphoma. J Nucl Med 41: 952-958, 2000.
14. Rose LM, Gunasekera AH, DeNardo SJ, DeNardo GL and Meares CF: Lymphoma-selective antibody Lym-1 recognizes a discontinuous epitope on the light chain of HLA-DR10. Cancer Immunol Immunother 43: 26-30, 1996.
15. Rose LM, Deng CT, Scott S, Xiong CY, Lamborn KR, Gumerlock PH, DeNardo GL and Meares CF: Critical Lym-1 binding residues on polymorphic HLA-DR molecules. Mol Immunol 36: 789-797, 1999.
16. Epstein AL, Marder RJ, Winter JN, Stathopoulos E, Chen FM, Parker JW and Taylor CR: Two new monoclonal antibodies, Lym-1 and Lym-2, reactive with human-B-lymphocytes and derived tumors, with immunodiagnostic and immunotherapeutic potential. Cancer Res 47: 830-840, 1987.
17. Press OW, Farr AG, Borroz KI, Anderson SK and Martin PL: Endocytosis and degradation of monoclonal antibodies targeting human B-cell malignancies. Cancer Res 49: 4906-4912, 1989.
18. Tobin E, DeNardo GL, Zhang N, Epstein AL, Liu C and DeNardo SJ: Combination immunotherapy with anti-CD20 and anti-HLA-DR monoclonal antibodies induces synergistic anti-lymphoma effects in human lymphoma cell lines. Leuk Lymphoma 48: 944-956, 2007.
19. Liu C, De Nardo GL, Tobin E and De Nardo SJ: Antilymphoma effects of anti-HLA-DR and CD20 monoclonal antibodies (Lym-1 and rituximab) on human lymphoma cells. Cancer Biother Radiopharmaceut 19: 545-561, 2004.
20. Ottonello L, Morone P, Dapino P and Dallegri F: Monoclonal Lym-1 antibody-dependent lysis of B-lymphoblastoid tumor targets by human complement and cytokinine-exposed mononuclear and neutrophilic polymorphonuclear leukocytes. Blood 87: 3262-3269, 1996.
21. Balhorn R, Hok S, Burke P, Lightstone FC, Cosman M, Zemla A, Mirick GR, Perkins J, Natarajan A, Corzett M, De Nardo SJ, Lehner H, Albrecht H, Gregg JP and De Nardo GL: Selective high affinity ligand (SHAL) 'antibody mimics' for cancer diagnosis and therapy: initial application to lymphoma/leukemia. Clin Cancer Res (In press).

22. West J, Perkins J, Hok S, Balhorn R, Lightstone FC, Cosman M, DeNardo SJ and DeNardo GL: Direct antilymphoma activity of novel, first-generation 'antibody mimics' that bind HLA-DR10-positive non-Hodgkin's lymphoma cells. Cancer Biother Radiopharm 21: 645-654, 2006.
23. DeNardo GL, Natarajan A, Hok S, Perkins J, Cosman M, DeNardo SJ, Lightstone FC, Mirick G, Miers LA, Yuan A, Xiong CY and Balhorn R: Pharmacokinetic characterization in xenografted mice of a series of first generation mimics for HLA-DR antibody, Lym-1, as carrier molecules to image and treat lymphoma. J Nucl Med (In press).
24. Scatchard G: The attraction of proteins for small molecules and ions. Ann NY Acad Sci 51: 660-666, 1947.
25. Kuntz ID, Blaney JM, Oatley SJ, Langridge R and Ferrin TE: A geometric approach to macromolecule-ligand interactions. J Mol Biol 161: 269-288, 1982.
26. Desjarlais RL, Sheridan RP, Seibel GL, Dixon JS, Kuntz ID and Venkataraqhavan R: Using shape complementarity as an initial screen in designing ligands for a receptor binding site of known three-dimensional structure. J Med Chem 31: 722-729, 1988.
27. Hok S, Natarajan A, Balhorn R, DeNardo SJ, DeNardo GL and Perkins J: Synthesis and radiolabeling of selective high affinity ligands designed to target non-Hodgkin's lymphoma and leukemia. Bioconjug Chem 18: 912-921, 2007.
28. Fand I and McNally WP: The technique of whole-body autoradiography. In: Current Trends in Morphological Techniques. 1st edition. Johnson JE (ed). CRC Press, Boca Raton, FL, pp1-28, 1981.
29. DeNardo GL, Kroger LA, DeNardo SJ, Miers LA, Salako Q, Kukis DL, Fand I, Shen S, Renn O and Meares CF: Comparative toxicity studies of yttrium-90 MX-DTPA and 2-IT-BAD conjugated monoclonal antibody (BrE-3). Cancer 73: 1012-1022, 1994.
30. Hollander M and Wolfe DA: Non-Parametric Statistical Methods. Wiley, New York, 1973.
31. CRC Handbook of Tables for Probabilities and Statistics. 2nd edition. CRC Press, Boca Raton, FL, 1968.
32. Mammen M, Choi S-K and Whitesides GM: Polyvalent interactions in biological systems: implications for design and use of multivalent lligands and inhibitors. Angew Chem Int Edit 37: 2755-2794, 1998.
33. Kiessling LL, Gestwicki JE and Strong LE: Synthetic multivalent ligands in the exploration of cell-surface interaction. Curr Opin Chem Biol 6: 696-703, 2000.
34. Fine HA, Figg WD, Jaeckle KA, Wen PY, Kyritsis AP, Athanassios P, Loeffler JS, Levin VA, Black PM, Kaplan R, Pluda JM, *et al*: Phase II trial of the antiangiogenic agent thalidomide in patients with recurrent high-grade gliomas. J Clin Oncol 18: 708-715, 2000.
35. Sutcliffe-Goulden JL, O'Doherty MJ, Marsden PK, Hart IR, Marshall JF and Bansal SS: Rapid solid phase synthesis and biodistribution of 18F-labelled linear peptides. Eur J Nucl Med Mol Imaging 29: 754-759, 2002.
36. Reilly RM, Sandhu J, Alvarez-Diez TM, Gallinger S, Kirsh J and Stern H: Problems of delivery of monoclonal antibodies. Pharmaceutical and pharmacokinetic solutions. Clin Pharmacokinet 28: 126-142, 1995.
37. Chen P, Wang J, Hope K, Jin L, Dick J, Cameron R, Brandwein J, Minden M and Reilly RM: Nuclear localizing sequences promote nuclear translocation and enhance the radiotoxicity of the anti-CD33 monoclonal antibody HuM195 labeled with $^{111}$In in human myeloid leukemia cells. J Nucl Med 47: 827-836, 2006.
38. Takeuchi T, Kosuge M, Tadokoro M, Sugiura Y, Nishi M, Kawata M, Sakai N, Matile S and Futaki S: Direct and rapid cytosolic delivery using cell-penetrating peptides mediated by pyrenebutyrate. ACS Chem Biol 1: 299-303, 2006.
39. Han K, Jeon MJ, Kim SH, Ki D, Bahn JH, Lee KS, Park J and Choi SY: Efficient intracellular delivery of an exogenous protein GFP with genetically fused basic oligopeptides. Mol Cell 12: 267-271, 2001.
40. Kim HH, Choi HS, Yang J-M and Shin S: Characterization of gene delivery *in vitro* and *in vivo* by the arginine peptide system. Int J Pharm 335: 70-78, 2007.
41. Lebl M, Krchnak V, Sepetov NF, Seligmann B, Strop P, Felder S and Lam KS: One-bead-one-structure combinatorial libraries. Biopolymers 37: 177-198, 1995.
42. Liu R, Marik J and Lam KS: Design, synthesis, screening, and decoding of encoded one-bead one-compound peptidomimetic and small molecule combinatorial libraries. Methods Enzymol 369: 271-287, 2003.